Bol. Soc. Paran. Mat.
©SPM – E-ISSN-2175-1188
SPM: www.spm.uem.br/bspm

(3s.) **v. 2026 (44) 3** : 1–12.
ISSN-0037-8712
doi:10.5269/bspm.79467

An Optimized Hybrid Mesh Adaptation Approach for Non-Stationary Problems Applied to Air Quality Modeling

Hatim TAYEQ, Anouar EL HARRAK and Amal BERGAM

ABSTRACT: In this work, we propose a novel idea that optimizes self-adaptation algorithms for unstructured meshes of domains with complex geometries, applied to nonstationary problems. This idea allows for adapting the spatial mesh at self-detectable instants, according to the values of a parameter calculated as a function of both spatial and temporal indicators. In this algorithm, spatial mesh adaptation using our new approach uses specific strategies of refinement and de-refinement. We validate the efficiency of the proposed algorithm through an air quality forecasting application, employing a numerical model governed by the parabolic PDE of advection-diffusion-reaction type, to forecast sulfur dioxide (SO_2) concentrations. The application focuses on a local scale, specifically the Grand Casablanca area (Morocco), using real meteorological data to estimate the PDE parameters.

Key Words: Self-adaptive algorithms, a posteriori error estimates, air quality forecasting, sulfur dioxide dispersion, finite volume method, mesh adaptation.

Contents

1. Introduction

Error estimation based on the a posteriori analysis for nonstationary problems often presents immense difficulties, due to the presence of two discretization meshes, time and space.

In [19], Johnson et al. established error versus time indicators for a parabolic problem. Another concept for the a posteriori analysis of parabolic problems consists of giving spatial error indicators; in this context, we refer to the works of Bieterman and Babuska [9,10], Picasso [25], Bergam et al. [5,7]. The last concept is to provide indicators compared to the both discretizations, in space and time, in this context, we cite Verfurth's work [34,35].

In general, a posteriori error estimation aims to develop local indicators used to implement some self-adaptive algorithms to reduce computational cost and used resources in the numerical resolution, and also to improve the approximate solution. Recently, particular attention has been brought to self-adaptive algorithms as a robust tool to reduce the calculation costs of numerical simulation. Indeed, numerical simulation using mesh self-adaptive algorithms minimizes the number of elements without losing the quality of the solution.

The same problem arises during the mesh self-adaptation for the parabolic problems. In practice, self-adaptation either takes place in space (based on the values of the spatial indicator as in [3,8,26,32]), or in time (based on the values of the temporal indicator, as in the work of S. Gustaf [30]).

2020 *Mathematics Subject Classification:* 58F15, 58F15, 53C35.
Submitted November 05,2025. Published February 22, 2026

For that, in this paper, we apply a novel self-adaptive algorithm named: *Hybrid self-adaptive algorithm*, noted *HSAA*. The proposed approach is based on a new technique of unstructured mesh adaptation by introducing a parameter given in terms of both error indicators (spatial and temporal). Even more, this parameter is simply calculable and will be used to mark candidate instants for spatial mesh adaptation, to avoid mainly mesh adapting at each iteration of time. Furthermore, an example is provided to emphasize and validate the efficiency of *HSAA*. In this example, we used a real application concerning the non-stationary numerical model to forecast the sulfur dioxide (SO_2) concentrations in the air at a local scale over the Grand Casablanca area represented by a complex geometry domain. Where we validate the efficiency of the new algorithm compared to the classical one applied to parabolic problems. We show that our new algorithm is more effective and faster.

Hence, our idea minimizes the number of candidate instants for mesh adaptation, and t allows for the reduction of the corresponding CPU time, which guarantees a good quality solution and a better use of available computing resources. Moreover, *HSAA* ensures a balance between the error relating to the temporal discretization and that due to the spatial discretization, because we use specific strategies of refinement and de-refinement.

As the problem treated in this work comes from the conservation laws, it is necessary to take the conservative aspect of the model during the numerical resolution. This is why we used a numerical method taking this aspect into consideration, which is the finite volume method of type vertex-centered with the Euler implicit scheme in time. This choice ensures the stability of the numerical scheme like that used in [4,11,16,33]. We note that our approach applies to all numerical methods based on spatio-temporal meshes.

In the rest of this paper, we describe in section 2 two self-adaptive algorithms, the classical and *HSAA*. Hereinafter, in section 3, we present the numerical model forecasting the sulfur dioxide in the air and the definition of the error indicators of the treated problem. Finally, in section 4, we give the numerical and simulation results forecasting SO_2 over the Grand Casablanca area (Morocco), using real meteorological data provided by the General Directorate of Meteorology of Morocco (DGM). Those results show the reliability and efficiency of our new self-adaptive mesh algorithm dedicated to parabolic problems.

2. Hybrid self-adaptive algorithm

2.1. Idea of Hybrid self-adaptive algorithm

Self-adaptation of spatial mesh is often based on the use of spatial error indicator as an adaptation criterion, to ensure that the relative error (using a given norm) between the discrete solution and the exact one is less than a predefined tolerance $\varepsilon > 0$. This classical strategy mainly aims to locally control the error and to equilibrate the error over each part of the spatial domain by refining or de-refining some regions.

A major disadvantage of the classical strategy may appear at the execution level. Indeed, if the prescribed tolerance ε is very small, the algorithm may require a high computation time and may enter a very long loop to ensure the control of the error. Unfortunately, it is a waste of time to perform a spatial mesh adaptation strategy at each iteration since the error basically occurred due to both temporal and spatial discretization. If the error is dominated by time discretization, so there is no need to perform a spatial mesh adaptation strategy because it is a waste of time rather than a gain in precision. Thus, to maintain a balance between temporal discretization and spatial one, we will perform a spatial mesh adaptation strategy at specified iterations according to a calculable parameter, so that we can reduce computational cost without losing the precision of the approximate solution.

o this end, we will use both spatial and temporal indicators to calculate a parameter λ_h^n which indicates the iterations $t_i \in [t_0, t_N]$ in which we will adapt the spatial mesh. The parameter λ_h^n is defined as follows:

$$\lambda_h^n = \frac{\theta_h^n}{\eta_h^n}, \tag{2.1}$$

where η_h^n is the spatial indicator, and θ_h^n is the temporal one defined in subsection 3.2.1 by 3.6 and 3.7.

Hybrid self-adaptive algorithm takes into account the values of λ_h^n (given by 2.1), so that it performs the spatial mesh adaptation only if $\lambda_h^n > \widetilde{\lambda}$ where $\widetilde{\lambda}$ is the value of λ_h^n calculated in the last iteration

where we performed spatial mesh refinement strategy.

In Table 1, we present the classical algorithm which takes into consideration just the spatial indicator. This algorithm was subject to several works [2,6,33] and others. Table 2 presents our novel *HSAA*.

Table 1: Classical Algorithm: Traditional approach.

	Classical Algorithm:
Step 1:	Input pre-processing data: Problem data and ε.
Step 2:	Generate the mesh (primal and dual).
Step 3:	Solve the discrete problem at instant t_n.
Step 4:	Compute the local spatial error indicator for each element in spatial mesh.
Step 5:	Compute the global error indicator η_h^n.
Step 6:	If $\eta_h^n \leq \varepsilon$, then Go to Step 3 at instant t_{n+1}. Else Go to Step 7.
Step 7:	Adapting the spatial mesh, then Go to Step 3.

Table 2: *Hybrid self-adaptive algorithm*: Our novel approach.

	Hybrid self-adaptive algorithm:
Step 1:	Input pre-processing data: Problem data and ε, and ε'. Setting **Updating:=TRUE**.
Step 2:	Generate the mesh (primal and dual).
Step 3:	Solve the discrete problem at instant t_n.
Step 4:	Compute spatial and temporal indicators. Calculate the parameter λ_h^n. If **Updating=TRUE**, then set $\tilde{\lambda} := \lambda_h^n$ and **Updating:=FALSE**.
Step 5:	If $\frac{\lambda_h^n - \tilde{\lambda}}{\tilde{\lambda}} > \varepsilon'$ then Go to Step 6. Else Go to Step 3 at instant t_{n+1}.
Step 6:	If the calculated global error indicator $\eta_h^n \leq \varepsilon$, then Go to Step 3 at instant t_{n+1}. Else Go to Step 7.
Step 7:	Adapt the spatial mesh, setting **Updating:=TRUE**, and then Go to Step 3.

2.2. Marking strategy and adaptation techniques

To adapt the spatial mesh, it is necessary to choose which mesh elements must be refined or de-refined. For this, we chose the following strategies to perform those tasks, namely marking, refinement, and de-refinement.

Marking strategy: Here, we use Dorfler's strategy [13], called *Guaranteed Error Reduction Strategy* to reduce the error at each adaptation level [14].

Refinement technique: For triangular meshes, there are essentially two refinement techniques to preserve the regularity of the mesh:

Technique 1: We divide a triangle T into two triangles T_1 and T_2 by constructing the median of the triangle relative to the longest edge (Figure 1-a).

Technique 2: We divide the triangle T into 4 triangles T_1, T_2, T_3 and T_4 by joining the midpoints of its edges (Figure 1-b). This technique is given in [29], it has the advantage that the new triangles $(T_i)_{i=1,\ldots,4}$ are geometrically similar to the triangle T.

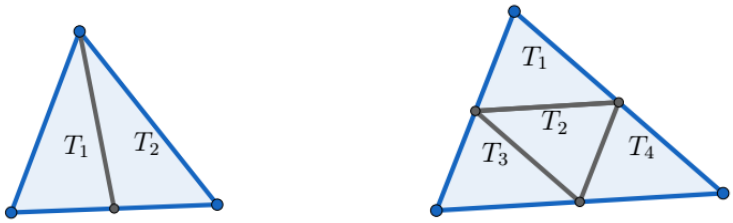

(a) (b)

Figure 1: Refinement techniques: (a) Technique 1, (b) Technique 2

De-refinement technique: In order to preserve the regularity of the mesh elements, an element is de-refined only if it comes from a previous refinement level. Furthermore, the elements of the initial mesh can not be de-refined to keep a certain level of regularity. The de-refinement process is an inverted refinement that consists of merging two triangles (or 4 triangles) resulting from a refinement to remove a node (or nodes).

In the following, we present the numerical results of air quality application proving the effectiveness of our approach using the finite volume method.

3. Numerical model forecasting the sulfur dioxide in the air

Climate change is one of the biggest threats to our environment. According to WHO annual reports [24], air pollution is the major factor causing this phenomenon and is a "public health emergency", because more than 90% of the world's population is exposed to toxic air [23]. This pollution mainly affects the atmospheric boundary layer [31]. Among the pollutants emitted directly into the air, we find sulfur dioxide (SO_2) which is a pollutant causing global warming. Its emission in the urban atmosphere comes mainly from the burning of fossil fuels, factories, and road traffic [1]. SO_2 is a colorless gas and flammable with a pungent smell that irritates the eyes and respiratory tract. The increase in sulfur dioxide concentration may cause dramatic consequences such as diseases and death if no action is taken.

During the last few years, there has been a lot of interest in forecasting pollutant concentrations in the air and studying air quality as well. In this context, we use the diffusion-advection-reaction partial differential equation (PDE) to forecast SO_2 concentration which represents our main problem [15,28]. To this end, we usually use numerical methods to build approximate models that are easier to handle and implement. To approximate the solution of our problem we use the Adaptive Vertex-Centered Finite Volume Method (AVCFVM) with the backward Euler scheme in time.

Problem statement: The mathematical model of SO_2 dispersion in the first layer of the atmosphere is given by the non-stationary PDE 3.1 [15,28]:

$$\underbrace{\frac{\partial c}{\partial t}}_{Accumulation} + \underbrace{\operatorname{div}(cV)}_{Advection} - \underbrace{\operatorname{div}(D\nabla c)}_{Diffusion} + \underbrace{rc}_{Reaction} = \underbrace{f}_{Source}, \tag{3.1}$$

where, $\partial c/\partial t$ is the accumulation of SO_2 concentration. c is SO_2 concentration in $[kg.m^{-3}]$.

We denote the advection mechanism by $\operatorname{div}(cV)$. The term $\operatorname{div}(D\nabla c)$ represents the diffusion mechanism, where D is the diffusion matrix in $[m^2.s^{-1}]$. V represents the vector of wind velocity given by $[m.s^{-1}]$. Finally, rc is the reaction term modeling the pollutant production by chemical reactions. Furthermore, the last term f is the source term given in $[kg.m^{-3}.s^{-1}]$.

In this paper, we used the simplified version of this model in two dimensions, because the main components of the wind are horizontal [20,36].

This model is completed by the initial condition $c_0 \geq 0$, and the appropriate boundary condition summarized in the following system:

$$\begin{cases} \frac{\partial c}{\partial t}(x,t) + \operatorname{div}(cV)(x,t) - \operatorname{div}(D\nabla c)(x,t) + rc(x,t) = f(x,t), \ (x,t) \in \Omega \times]0,T] \\ D\frac{\partial c}{\partial n}(x,t) = 0, \quad (x,t) \in \partial\Omega \times [0,T], \\ c(x,0) = c_0, \quad x \in \Omega, \end{cases} \tag{3.2}$$

where T is a final positive time ($0 < T < \infty$), and $\Omega \subset \mathbb{R}^2$ is a bounded real domain with regular boundary $\partial\Omega$. n is the unit normal vector oriented outward from $\partial\Omega$. The choice of the boundary condition in this work is due to the model construction in which conservation laws were applied [21,22]. In our case, this condition relates the flux only with the density along the boundary, without external factors.

D, V, r and f satisfy the necessary conditions for the problem to be well-posed.

Using the standard Sobolev space notation, we assume that (conditions imposed by the a posteriori analysis of the error):

There exist two constants $\alpha \geq 0$ and $\beta \geq 0$ such that

$$\frac{1}{2}\operatorname{div} V + r \geq \beta, \text{ and } \|r\|_{L^\infty(\Omega)} \leq \alpha\beta \text{ in } [0,T].$$

We assume that D is a function satisfying [17]:

$$0 \leq D(x,t) \leq 1, \quad \forall (x,t) \in \Omega\times]0,T].$$

3.1. Numerical approximation of the air quality model

In this section, we apply an Adaptive Vertex-Centered Finite Volume Method (AVCFVM) discretization to the problem (3.2), which governs the transport of the pollutant SO_2. This choice is judicious given the conservative characteristics of the problem.

In the rest of the paper, $\forall c \in L^2\big(0,T;H^1(\Omega)\big)$, we define the energy norm:

$$[[c]](t) = \{\|c(t)\|^2_{0,\Omega} + \int_0^t |||c(s)|||^2 ds\}^{1/2},$$

such as:

$$|||c||| = \{\|D^{1/2}\nabla c\|^2 + \beta\|c\|^2_0\}^{1/2}.$$

The weak formulation of the Problem (3.2) is given by:

$$(WF)\begin{cases} \text{Find } c \in L^2\big(0,T;H^1(\Omega)\big) \text{ satisfying for every } v \text{ in } H^1(\Omega) \\ \displaystyle\int_\Omega \frac{\partial c}{\partial t} v dx + \int_\Omega D\nabla c\cdot\nabla v dx + \int_\Omega \operatorname{div}(cV)v dx + \int_\Omega rcv dx = \int_\Omega fv dx, \\ c(.,0) = c_0. \end{cases} \tag{3.3}$$

The problem (3.3) admits a unique solution [12,18,27].

The AVCFVM requires a discretization of the space Ω and also the time domain $[0,T]$. The temporal mesh of $[0,T]$ is given by N sub-intervals such that: $0 = t_0 \leq t_1, \ldots, \leq T = t_N$. We set $\tau_n = t_n - t_{n-1}$, $\forall n = 1,\ldots,N$.

For each t_n, we associate a partition $\mathcal{T}_h^n$ of the space Ω, which is formed by M closed triangles K. Also, we denote by $\mathcal{V}_h^n$ the Vertex-centered dual mesh associated to $\mathcal{T}_h^n$. The mesh $\mathcal{V}_h^n$ is formed by M_n volumes V_i (shown in Figure 2).

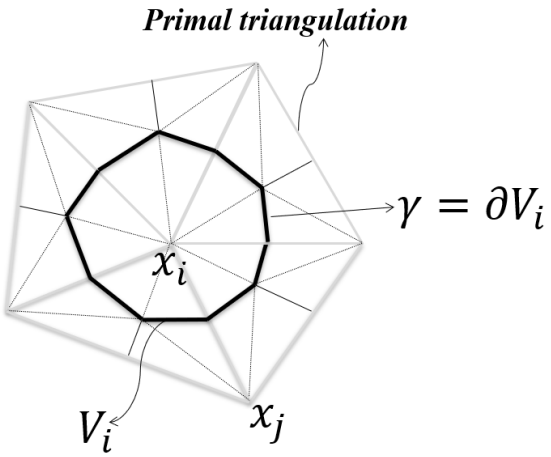

Figure 2: Vertex-centred mesh in two dimensions

We introduce the Backward Euler scheme for the derivative with respect to time:

$$\frac{c^n(x) - c^{n-1}(x)}{\tau_n} + \operatorname{div}(c^n V^n)(x) - \operatorname{div}(D^n \nabla c^n)(x) + r c^n(x,t) = f^n(x), \quad x \in \Omega, \tag{3.4}$$

where c, D, f and V are evaluated with respect to time at instant t_n.

Furthermore, we integrate equation (3.4) over each control volume $V_i \in \mathcal{V}_h^n,\ i = 1, \ldots, N$, we get the following finite volume discretization of Problem (3.2):

$$\int_{V_i} \frac{c^n(x) - c^{n-1}(x)}{\tau_n} dx - \int_{V_i} \Big(\operatorname{div}\left(D^n \nabla c^n(s)\right) - \operatorname{div}(c^n V^n)(s) \Big) dx + \int_{V_i} r c^n(x) dx = \int_{V_i} f^n(x) dx,$$

Then, using the Green formula, we get

$$\int_{V_i} \frac{c^n(x) - c^{n-1}(x)}{\tau_n} dx - \sum_{\gamma \in \partial V_i \setminus \partial\Omega} \int_\gamma \left\{ D^n \nabla c^n(s) - c^n(s) V^n \right\}.n_\gamma ds + \sum_{\gamma \in \partial V_i \cap \partial\Omega} \int_\gamma c^n(s) V^n.n_\gamma ds + \int_{V_i} r c^n(x) dx = \int_{V_i} f^n(x) dx,$$

where ∂V_i is the boundary of the control volume $V_i,\ i = 1, \ldots, N$ (See Figure 2).

We denote by n_γ the unit outer-normal vector on ∂V_i, and $\gamma \in \partial V_i \cap \partial\Omega$.

We define the approximate finite-dimensional space $X_{(\Omega,h)}$ by

$$X_{(\Omega,h)} := \left\{ v_h \in \mathcal{C}^0(\overline{\Omega}) : \forall K \in \mathcal{T}_h^n,\ v_h|_k \in \mathcal{P}_1 \right\},$$

where $\mathcal{P}_1$ is the set of polynomial functions of degree ≤ 1.

Let $(\psi_i^n)_{i=1\ldots N_n}$ be the basis functions of $X_{(\Omega,h)}$, allowing to write the $c_h^n \in X_{(\Omega,h)}$ as follows:

$$c_h^n = \sum_{i=1}^{M_n} \psi_i^n c_i^n,$$

where c_i^n are the approximate values of c^n in the control volume V_i.

Then, the numerical flux could be defined as:

$$\int_\gamma D^n \nabla c^n . n_\gamma ds \simeq \int_\gamma D_h^n \nabla c_h^n . n_\gamma ds \text{ and } \int_\gamma c^n V^n . n_\gamma ds \simeq \int_\gamma c_h^n V_h^n . n_\gamma ds,$$

where D_h, V_h and r_h are respectively piecewise polynomial approximations of D, V and r, such that there exists two constants c_1 and c_2 only depending on D and r respectively, satisfying

$$\|D - D_h\|_{L^\infty(\Omega)} \leq c_1 h^{l+1}, \text{and } \|r - r_h\|_{L^\infty(\Omega)} \leq c_2 h^{l+1}.$$

Hence, we obtain

$$\int_{V_i} \frac{c_h^n - c_h^{n-1}}{\tau_n} dx - \sum_{\gamma \in \partial V_i \setminus \partial\Omega} \int_\gamma \left\{ D_h^n \nabla c_h^n - c_h^n V_h^n \right\} . n_\gamma ds + \sum_{\gamma \in \partial V_i \cap \partial\Omega} \int_\gamma c_h^n V_h^n . n_\gamma ds + \int_{V_i} r_h c_h^n dx = \int_{V_i} f_h^n dx,$$

where f_h is a piecewise polynomial approximation of f.

The full discrete problem associated to Problem (3.2) is given by:

$$(P') \begin{cases} \textit{Find the family } (c_h^n)_{1 \leq n \leq N},\ c_h^n \in X_{(\Omega,h)},\ n = 1, ..., N, \textit{satisfying}: \\ \int_{V_i} \frac{c_h^n - c_h^{n-1}}{\tau_n} dx - \sum_{\gamma \in \partial V_i \setminus \partial\Omega} \int_\gamma \left\{ D_h^n \nabla c_h^n - V_h^n c_h^n \right\} . n_\gamma ds \\ \quad + \sum_{\gamma \in \partial V_i \cap \partial\Omega} \int_\gamma c_h^n V_h^n . n_\gamma ds + \int_{V_i} r_h c_h^n dx = \int_{V_i} f_h^n dx, \\ \text{for } i = 1, 2, ..., M_n. \end{cases} \tag{3.5}$$

3.2. A posteriori error analysis

Several works have been geared toward a posteriori error analysis, as a powerful method for mesh self-adaptation over the last decades. Indeed, a posteriori error analysis is intended to control errors between discrete and analytical solutions using calculable quantities called local indicators of the error.

The AVCFVM requires another discretization of the domain Ω noted $\mathcal{Q}_h^n$ formed by the polygonal $Q_{i,j}$ such that $Q_{i,j} = V_i \cap T_j$ where $T_j \in \mathcal{T}_h^n$ and $V_i \in \mathcal{V}_h^n$.

3.2.1. Indicators definition: In the following, we present the developed indicators of the error related to temporal and spatial discretizations.

First, we define *the spatial error indicator* by:

Definition 3.1

$$(\eta_h^n)^2 := \sum_{V \in \mathcal{V}_h^n} \sum_{Q \subset V} \alpha_Q^2 \| f_h^n - \frac{c_h^n - c_h^{n-1}}{\tau_n} + \text{div}(D_h^n \nabla c_h^n - c_h^n V_h^n) - r_h c_h^n \|_{0,Q}^2$$

$$+ D_{min}^{-1/2} \sum_{E \in \mathcal{E}_h^n} \alpha_E \left\| \left[D_h^n \frac{\partial c_h^n}{\partial n_E} \right]_E \right\|_{0,E}^2, \tag{3.6}$$

such that $\alpha_Q = min(h_Q D_{min}^{-1/2}, \beta^{-1/2})$ *and* $\alpha_E = min(h_E D_{min}^{-1/2}, \beta^{-1/2})$. h_Q *and* h_E *are respectively the diameter of* Q *and* E.

The temporal error indicator, which measures the error due to the discretization of the time interval, is given by:

Definition 3.2

$$(\theta_h^n)^2 := \frac{\tau_n}{3}\Big(\|(D_h^n)^{1/2}\nabla(c_h^n - c_h^{n-1})\|_{0,\Omega}^2 + \|\operatorname{div}\left((c_h^n - c_h^{n-1})V_h^n\right)\|_{0,\Omega}^2$$

$$+\|(r_h)^{1/2}(c_h^n - c_h^{n-1})\|_{0,\Omega}^2\Big). \tag{3.7}$$

The interpolation error $\mu_h^n(t)$ is given by:

Definition 3.3

$$\mu_h^n(t) := \max\left(\beta^{-1/2}, D\beta_{min}^{-1/2}\right)\Big(\|f - f_h^n + \operatorname{div}(c_{h,\tau t}(V_h^n - V)) + (r_h - r)c_{h,\tau t}\|_{0,\Omega}$$

$$+\|(D_h^n - D)\nabla c_{h,\tau t}\|_{0,\Omega}\Big), \tag{3.8}$$

where $c_{h,\tau t}$ *is an interpolation of* $(c_h^n)_n$, $n = 0, \ldots, M_n$, $\forall t \in [0,T]$, *which given by:*

$$\tau_n c_{h,\tau t}(x) := \tau_n c_h^{n-1}(x) + (t - t_{n-1})\big(c_h^n(x) - c_h^{n-1}(x)\big),\ \forall x \in \Omega \text{ and } t \in [t_{n-1}, t_n].$$

3.2.2. Upper bound for the error: The following theorem gives the upper bound of the error according to the predefined indicators.

Theorem 3.1 *Let* c *be the analytical solution of (3.2). Then,* $\exists\ \mathcal{C} > 0$*constant, independent of* h *and* τ, *such that:*

$$[[c - c_{h,\tau t}]](t_n) \leq \mathcal{C}\Big\{\|c_0 - \Pi_0 c_0\|_{0,\Omega}^2 + \sum_{m=1}^{n}\left((\tau_m \eta_h^m)^2 + (\theta_h^m)^2 + \int_{t_{m-1}}^{t_m} |\mu_h^n(t)|^2\right)\Big\}^{1/2}, \tag{3.9}$$

where η_h^n, θ_h^n, *and* μ_h^n *are defined by (3.6), (3.7), and (3.8), respectively.* Πc_0 *is the* L^2*-projection of* c_0 *on* $X_{(\Omega,h)}$.

We find the proof of this error estimation in [4] applied to porous media.

The resolution and numerical simulation by the AVCFVM method based on the indicators and a posteriori analysis presented in this section is the subject of the next section.

4. Numerical results and simulations

Here, we show the numerical results where we compare our novel self-adaptive algorithm with the classical one. We apply and validate our approach to forecast the sulfur dioxide concentrations in the atmospheric boundary layer over the Grand Casablanca area using real meteorological data obtained from the DGM (General Directorate of Meteorology) of Morocco.

Unfortunately, Morocco remains among the most important sources of sulfur dioxide in the world [23]. According to the WHO warning, the Kingdom of Morocco ranks among the countries where air pollution is higher than its recommendations. Also, in Greenpeace's turn, Morocco is ranked among the 25 source countries of SO_2 emissions. In particular, the Grand Casablanca area records pollution levels four times higher than those recommended by WHO. Since, as a real application, we choose Ω as the Grand Casablanca area to validate our approach (Figure 3). To perform this application, we rely on real available meteorological data from July 13, 2019, to simulate the parameters of our problem.

In Table 3, we give the list of data used to calculate the model parameters and to perform the numerical simulation. We calculate the diffusion coefficient D in the air using the formula given in [17]. We also assume that the initial concentration the sulfur dioxide over the entire area is punctual from a factory chimney, since 98% of SO_2 emissions come from industrial sectors in the Grand Casablanca area.

Table 3: Parameters of the numerical model, where $\mathbb{T}$ is the temperature and $\mathbb{P}$ is the pressure.

Parameter	Signification	Value
D	Diffusion coefficient [17]	$D = 0.004832\frac{\mathbb{T}^{1.75}}{\mathbb{P}}\ cm^2 s^{-1}$
V	Velocity vector	given by wind speed and directions
r	Reaction coefficient	represents 2% of present pollutant
c_0	Initial concentration	$0\ \mu g.m^{-3}$

We apply *HSAA* to reduce computational cost while maintaining the accuracy of the approximate solution. Indeed, to present the efficiency of our approach, we give a comparison result between *HSAA* and the classical one. We will show the impact of *HSAA* on the number of iterations in which spatial mesh refinement strategy is applied, and thus on CPU time too.

Figure 3(a) shows the study domain (GCA) discretized by a primal mesh constructed by a finite element triangulation 3(b).

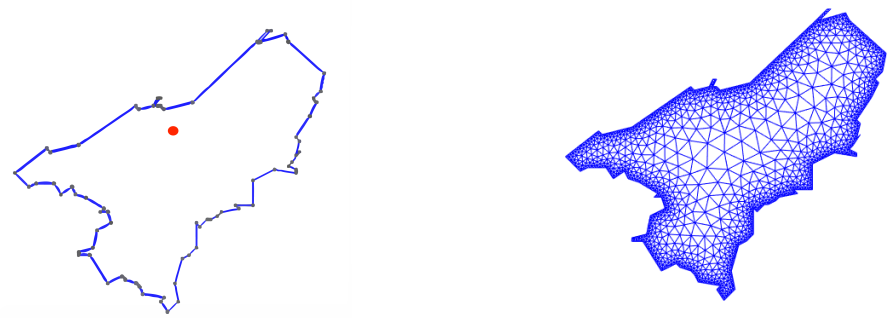

(a) (b)

Figure 3: Grand Casablanca Area (a), Adaptive mesh of GCA (b), • is the source position.

In Figures 4, we have shown the approximate solution at three times in the last spatial adaptation level, and in Figure 5 we show the associate adaptive mesh obtained by *HSAA* in the same times. We note that the approximate solution represents the concentration of SO_2 on GCA at any time ($t \in [0, T]$).

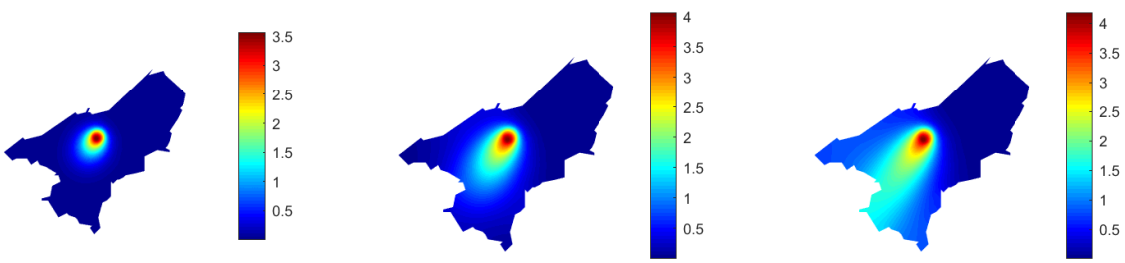

(a) (b) (c)

Figure 4: Approximate solution of Problem (3.2) at three times: a: $t = 10$, b: $t = 30$ and c: $t = 100$

To obtain a good approximation of the solution using the classical algorithm, we must perform a spatial mesh refinement strategy at each iteration, which is a CPU time-consuming technique. However, in *HSAA*, the spatial refinement parameter allows us to detect the distribution of time iterations where a spatial refinement strategy is necessary to be applied. Therefore, we can obtain an accurate solution with fewer spatial adaptation iterations of spatial mesh adaptation.

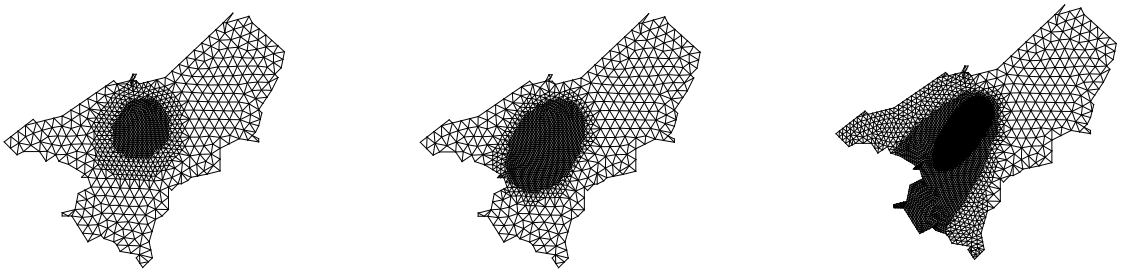

(a) (b) (c)

Figure 5: Adaptive mesh in the last adaptation level and the associate approximate solution of Problem (3.2) at three times: a: $t = 10$, b: $t = 30$ and c: $t = 100$

Table 4 shows a comparison of the number of iterations during which the spatial adaptation strategy is performed between the classical algorithm and the *HSAA*. We report the total number of triangles from the first to the last instant (overall adaptation levels). The comparison of the results is performed in relation to the full refinement method where the spatial adaptation process is stopped soon after the same achieved level of accuracy is reached. Moreover, the discretization of the time interval was taken to be regular, with a time step specifically adapted to the numerical solution method, thereby ensuring the stability of the approximate solution. In this context, the *HSAA* showed a clear improvement over the classical approach in terms of the efficiency and frequency of spatial refinement.

Table 4: Comparison of total iterations number at three times where a spatial adaptation strategy is applied between classical Algorithm and *Hybrid self-adaptive algorithm*.

Resolution strategy	Total adaptation iteration at		
	$t = 10$	$t = 30$	$t = 100$
CMA	1000	3000	10000
HSAA	472	1315	4286

with: CMA: Classical Mesh Adaptation.

One can notice that the *HSAA* allows us to significantly reduce the number of iterations in which spatial adaptation is performed. Consequently, the overall computational cost is also considerably reduced. Moreover, this technique enables us to reach the same level of accuracy as that obtained with a fully refined mesh, while requiring substantially fewer computational resources. This clearly highlights the efficiency of the proposed approach in maintaining solution quality with optimized performance.

Conclusion

In conclusion, problems using complex data such as meteorological and air quality data require special handling, especially if the solution domain is geometrically complex. Otherwise, the manipulation of the data and the resolution of the resulting problems require a very high computational time. For that, in this work, we proposed a novel technique that incorporates the temporal indicator into the mesh adaptation strategy. The idea is proved by applying it to approximate the solution of a parabolic problem using

numerical methods. Our approach significantly reduced the number of iterations where we performed a spatial adaptation and also the computational cost.

The numerical simulation revealed and validated the importance and efficiency of our new approach, where we see that the computation time has been significantly reduced while keeping the good quality of the approximate solution. We note that the *HSAA* developed in this work is applicable not only to the finite volume method, but also for the finite element method and other numerical methods.

Moreover, it is possible to use this technique to develop new algorithms for adaptive time discretization, which will be very important and useful specifically when we solve concrete problems with huge dimensions in time and space. Air quality problems could be one of the most important applications of this study since in such an application one aims to achieve a global forecast of several species over a long period.

References

1. Aberdane, I and Gueraoui, K and Taibi, M and Ghouli, A and El Hammoumi, A and Cherraj, M and Kerroum, M and Walid, M and Fihri, O Fassi and Haddad, YM *Two-dimensional theoretical and numerical approach of pollutant transport in the lowest layers of the atmosphere*, International Review of Mechanical Engineering. 3(4) , (2009).
2. Afif, M and Bergam, A and Mghazli, Z and Verfurth, R *A posteriori estimators of the finite volume discretization of an elliptic problem*, Numerical Algorithms. 34, 127-136, (2003).
3. Agouzal, A and Maitre, J.M and Oudin, F *Un nouveau resultat d'estimation d'erreur pour les elements finis mixtes rectangulaires avec integration numerique.Aplication a l'Analyse de schemas de type Volumes Finis*, C. R. Acad. Sci.Paris. T.322, serie I, 1225-1229, (1996).
4. Amaziane, B and Bergam, A and El Ossmani, M and Mghazli, Z *A posteriori estimators for vertex centred finite volume discretization of a convection-diffusion-reaction equation arising in flow in porous media*, Int. J. Numer. Meth. Fluids. 59, 259-284, (2009).
5. Bergam, A and Bernardi, C and Hecht, F and Mghazli, Z *Error indicators for the mortar finite element discretization of a parabolic problem*, Numer. Algorithms. 34, 187-201, (2003).
6. Bergam, A and Bernardi, C and Mghazli, Z *A posteriori analysis of the finite element discretization of some parabolic equations*, Math. Comp. 251, 1117-1138, (2005).
7. Bergam, A and Chakib, Abdelkrim and Nachaoui, Abdeljalil and Nachaoui, Mourad *Adaptive mesh techniques based on a posteriori error estimates for an inverse Cauchy problem*, Applied Mathematics and Computation. 346, 865–878, (2019).
8. Bernardi, C and Metivet, B and Verfurth, R *Analyse numérique d'indicateurs d'erreur, in Maillage et adaptation*, George ed., Hermès.251-278, (2001).
9. Bieterman, M and Babuska, I *The finite element method for parabolic equations. I. A posteriori error estimation*, Numer. Math. 40, 339-371, (1982).
10. Bieterman, M and Babuska, I *The finite element method for parabolic equations. II. A posteriori error estimation and adaptive approach*, Numer. Math. 40, 373-406, (1982).
11. Chen, Chuanjun and Zhao, Xin *A posteriori error estimate for finite volume element method of the parabolic equations*, Wiley Online Library. 33(1), 259–275, (2017).
12. Dautray, R and Lions, J.L *Chap XVIII. Evolution Problems: Variational Methods, Math. Anal. and Numer. Methods Sci. Technology.*, Springer-Verlag, Heidelberg. 5, 467–680, (2000).
13. Dorfler, W.A *convergent adaptive algorithm for Poissons equation*, SIAM J. Numer. Anal. 33, 1106-1124, (1996).
14. Dorfler, W.A *Time and space-adaptive algorithm for the linear time dependent Schrodinger equation*, Numer. Math. 73, 419-448, (1996).
15. Ebrahimzadehab, E and Shahsavandc, A *Simulation of Environmental Pollution Due to SO2 Dispersion*, Energy Sources, Part A: Recovery, Utilization, and Environmental Effects. 36(19), 2095-2105, (2014).
16. El Harrak, Anouar and Tayeq, Hatim and Bergam, Amal *A posteriori error estimates for a finite volume scheme applied to a nonlinear reaction-diffusion equation in population dynamics*, DCDS-S, doi: 10.3934/dcdss.2021062. 14(7), 2183-2197, (2021).
17. Fish, B.R and Ridge, O and Jack, L *DIFFUSION COEFFICIENT OF SO2 IN AIR*, Envirmental letters. 2, 13-21, (1971).
18. Flotron, S and Rappaz, J *CONSERVATION SCHEMES FOR CONVECTION-DIFFUSION EQUATIONS WITH ROBIN BOUNDARY CONDITIONS*, Mathematical Modelling and Numerical Analysis. 47, 1765-1781, (2013).
19. Johnson, C and Nie, N.N and Thomee, V *An a posteriori error estimate and adaptive timestep control for a backward Euler discretization of a parabolic problem*, SIAM J. Numer. Anal. 27, 277-291, (1990).
20. Mallet, V and Pourchet, A and Quelo, D and Sportisse, B *Investigation of some numerical issues in a chemistry-transport model: Gas-phase simulations*, Journal of Geophysical Research. 112, 301-317, (2007).

21. Mallet, V and Sportisse, B *Uncertainty in a chemistry-transport model due to physical parameterizations and numerical approximations: An ensemble approach applied to ozone modeling*, Journal of Geophysical Research. 111, 1-15, (2006).

22. MIYAOKA, T.Y and MEYER, J.F.C.A and SOUZA, J.M.R *A General Boundary Condition with Linear Flux for Advection-Diffusion Models*, Tendências em Matemática Aplicada e Computacional. 18, 253-272, (2017).

23. *World Health Organization air pollution report 2016*, World Health Organization. (2016).

24. World Helth Organization *World Health Organization report 2 may 2018*, (2018).

25. Picasso, M *Adaptive finite elements for a linear parabolic problem*, Comput. Methods Appl. Mech. Engrg. 167, 223-237, (1998).

26. Qian, Yingzhi and Zhang, Xiaoping and Zhu, Yan and Ju, Lili and Guadagnini, Alberto and Huang, Jiesheng *A novel vertex-centered finite volume method for solving Richards' equation and its adaptation to local mesh refinement*, Journal of Computational Physics. 501, (2024).

27. Quarteroni, A and Valli, A *Numerical approximation of partial differential equations.*, Springer Series in Computational Mathematics. (1997).

28. Reynolds, SD and Roth, PM and Seinfeld, JH *Mathematical modeling of photochemical air pollution, Formulation of the model*, Atmospjeric Environnement. 7, 235-248, (1973).

29. Rivara, M.C *Mesh refinement processes based on the generalized bisection of simplices*, SIAM J. Numer. Anal. 21, 604–613, (1984).

30. Gustaf Soderlind and Lina Wang *Adaptive time-stepping and computational stability*, Journal of Computational and Applied Mathematics. 185(2), 225-243, (2006).

31. Stull, R.B *An introduction to boundary layer meteorology*, Kluwer Academic Publishers. (1998).

32. Tayeq, Hatim and El Harrak, Anouar and Bergam, Amal *A Posteriori Analysis of the Error for a Discontinuous Elliptic Problem*, Int. J. Appl. Comput. Math. 9(23), (2023).

33. Tayeq, Hatim and El Harrak, Anouar and Brgam, Amal and Khomsi, Kenza *Self-adaptive algorithm based on a posteriori analysis of the error applied to air quality forecasting using the finite volume method*, Discrete and Continuous Dynamical Systems Series S. 14(7), 2557-2570, (2020).

34. Verfurth, R *A posteriori error estimates for finite element discretizations of the heat equation*, Calcolo. 40, 195-212, (2003).

35. Verfurth, R *ROBUST A POSTERIORI ERROR ESTIMATES FOR NONSTATIONARY CONVECTION-DIFFUSION EQUATIONS*, SIAM J. NUMER. ANAL. 43, 1783-1802, (2010).

36. Wu, L and Mallet, V and Bocquet, M and Sportisse, B *A comparison study of data assimilation algorithms for ozone forecasts*, Journal of Geophysical Research. 113, 1-17, (2008).

Hatim TAYEQ,
Department of Mathematics,
Abdelmalek Essaadi University, Polydisciplinary Faculty of Larache. Larache,
Morocco.
ORCID iD: https://orcid.org/0000-0002-5988-650X
E-mail address: h.tayeq@uae.ac.ma

and

Anouar EL HARRAK,
Department of Mathematics,
Abdelmalek Essaadi University, Polydisciplinary Faculty of Larache. Larache,
Morocco.
ORCID iD: https://orcid.org/0000-0001-7608-5635
E-mail address: a.elharrak@uae.ac.ma

and

Amal BERGAM,
Department of Mathematics,
Abdelmalek Essaadi University, Polydisciplinary Faculty of Larache. Larache,
Morocco.
ORCID iD: https://orcid.org/0009-0008-1469-8194
E-mail address: abergam@uae.ac.ma